This article was downloaded by:
On: *26 January 2011*
Access details: *Access Details: Free Access*
Publisher *Taylor & Francis*
Informa Ltd Registered in England and Wales Registered Number: 1072954 Registered office: Mortimer House, 37-41 Mortimer Street, London W1T 3JH, UK

Liquid Crystals
Publication details, including instructions for authors and subscription information:
http://www.informaworld.com/smpp/title~content=t713926090

Temperature induced surface transitions in liquid crystal tilted homogeneous cells

R. Moldovan[a]; S. Frunza[a]; T. Beica[a]; M. Tintaru[a]
[a] Institute of Physics and Technology of Materials, Bucharest-Magurele, Romania

To cite this Article Moldovan, R. , Frunza, S. , Beica, T. and Tintaru, M.(1996) 'Temperature induced surface transitions in liquid crystal tilted homogeneous cells', Liquid Crystals, 20: 3, 331 — 335
To link to this Article: DOI: 10.1080/02678299608032042
URL: http://dx.doi.org/10.1080/02678299608032042

PLEASE SCROLL DOWN FOR ARTICLE

Full terms and conditions of use: http://www.informaworld.com/terms-and-conditions-of-access.pdf

This article may be used for research, teaching and private study purposes. Any substantial or systematic reproduction, re-distribution, re-selling, loan or sub-licensing, systematic supply or distribution in any form to anyone is expressly forbidden.

The publisher does not give any warranty express or implied or make any representation that the contents will be complete or accurate or up to date. The accuracy of any instructions, formulae and drug doses should be independently verified with primary sources. The publisher shall not be liable for any loss, actions, claims, proceedings, demand or costs or damages whatsoever or howsoever caused arising directly or indirectly in connection with or arising out of the use of this material.

LIQUID CRYSTALS, 1996, VOL. 20, NO. 3, 331–335

Temperature induced surface transitions in liquid crystal tilted homogeneous cells

by R. MOLDOVAN*, S. FRUNZA, T. BEICA and M. TINTARU
Institute of Physics and Technology of Materials, PO BOX MG 7, Bucharest-Magurele, 76900-Romania

(*Received 4 August 1995; accepted 26 October 1995*)

Temperature induced surface transitions in liquid crystal tilted homogeneous cells are experimentally studied. The results are theoretically explained by an elastic theory of surface transitions and the resulting values for the effective splay-bend elastic constant $\bar{k}_{13}$ for each liquid crystal material are compared with the results from experience with other types of surface anchoring.

Downloaded At: 09:23 26 January 2011

1. Introduction

The surface orientation of a nematic liquid crystal limited by a solid substrate or at the free surface is a function of the physical properties of the solid substrate and of the liquid crystal. The surface orientation may be stable or unstable with respect to temperature variation. If it is temperature dependent, the nematic sample shows a temperature dependent average molecular orientation [1–8], called a temperature induced transition. These temperature induced surface transitions have been recently explained by a new model [9] which takes into account the different temperature behaviours of the effective splay-bend and of the normal elastic constant [8–11]. According to the elastic model, the splay-bend elastic constant introduces a sharp variation of the nematic orientation near the surface, a variation also observed by Shen [12]. For tilted homogeneous samples with symmetrical anchoring of the liquid crystal at the two limiting surfaces, the equilibrium bulk tilt angle, measured from the normal to the substrate, Φ_b, is given by the equation [8]

$$\Phi_b = \Phi_0 - \frac{1}{2}\frac{\bar{k}_{13}}{k}\sin(2\Phi_0) \tag{1}$$

where Φ_0 is the equilibrium tilt angle at the limiting surface of the liquid crystal, $\bar{k}_{13}$ and k are the effective splay-bend [8] and the normal elastic constant (in the uni-constant approximation), respectively.

In the hypothesis of a strong anchoring, $\Phi_0 = \Phi_e =$ constant, where Φ_e is the easy direction of the Rapini–Papoular model [13]. On the contrary, for weak anchoring, the surface tilt angle Φ_0 is given by the equation:

$$\frac{\sin[2(\Phi_0 - \Phi_e)]}{\sin(4\Phi_0)} = \frac{L}{2b}\left(\frac{\bar{k}_{13}}{k}\right)^2. \tag{2}$$

In equation (2)

$$b = (k^*/k)^{1/2} \tag{3}$$

is a mesoscopic length, being the ratio between the second order elastic constant k^* and k, and

$$L = k/w \tag{4}$$

is the extrapolation length, being the ratio between k and w, the anchoring strength of the Rapini–Papoular part of the surface anchoring energy [13].

In the presence of a wall that tends to give either a homeotropic orientation ($\Phi_e = 0$) or a planar orientation ($\Phi_e = \pi/2$), the surface tilt angle is given by

$$\Phi_0 = \frac{1}{2}\arccos\left\{\pm\frac{b/L}{(\bar{k}_{13}/k)^2}\right\} \tag{5}$$

with the bulk tilt angle given by equation (1), when the modulus of the bracket in the right member of equation (5) is less than 1. In the opposite case, the equilibrium tilt angle is $\Phi_0 = 0$ and, consequently, $\Phi_b = 0$.

The temperature dependences of the usual elastic constant, k, and of the effective splay-bend elastic constant, $\bar{k}_{13}$, as well as that of the anchoring strength, w, were supposed to be [11]

$$\frac{\bar{k}_{13}}{k} = C + \frac{D}{(T_c - T)^{1/2}} \tag{6}$$

*Author for correspondence.

0267–8292/96 $12·00 © 1996 Taylor & Francis Ltd.

and

$$b\frac{w}{k} = A + \frac{B}{(T_c - T)^{1/2}} \tag{7}$$

where A, B, C and D are constants, T is the temperature in degrees Kelvin and T_c is a temperature a little higher than the nematic–isotropic transition temperature of the liquid crystal, T_{NI}. The ratio b is temperature independent [8]. Using these temperature dependences, the temperature dependence of the bulk tilt angle in the weak anchoring hypothesis is [11]

$$\begin{aligned}\Phi_b = \frac{1}{2}\arccos\left\{\frac{A + B/(T_c - T)^{1/2}}{[C + D/(T_c - T)^{1/2}]^2}\right\} \\ -\frac{1}{2}\left\{C + \frac{D}{(T_c - T)^{1/2}}\right\} \\ \times\left\{1 - \frac{[A + B/(T_c - T)^{1/2}]^2}{[C + D/(T_c - T)^{1/2}]^4}\right\}^{1/2}\end{aligned} \tag{8}$$

The experimental data presented in § 3 and measured as is described in § 2 were fitted either in the hypothesis of strong anchoring, by using equation (1) with $\bar{k}_{13}/k$ given by equation (6) and consequently, Φ_0, C and D as parameters, or, for weak anchoring, by using equation (8) with A, B, C and D as parameters. The anchoring type and the corresponding fitting parameters were chosen so that the values of $\bar{k}_{13}/k$ for the same liquid crystal material, for a variety of surface treatments and geometrical conditions, are in good agreement, as is shown in § 4.

2. Experimental

The samples used in the experimental investigations were prepared from planar glass plates, 1·7 mm thick, covered with a transparent conductive layer of indium tin oxide. The cell gap was assured by use of Mylar spacers, 15 μm thick, and was then measured by an interferometric method. Three types of surface treatment were used: (I) oblique deposition of an SiO_x layer at an incidence angle greater than 80°; (II) SiO_x double deposition at an angle greater than 80°, followed by a second deposition at an angle of 60° from the perpendicular direction; (III) oblique deposition of a SiO_x layer at an incident angle of 60°, combined with the effect of the surfactant ZLI 584 (E. Merck) dissolved in the liquid crystal for homeotropic alignment on the surface. The two glasses forming the cell, treated in the same manner, were mounted so that symmetrical boundary conditions were obtained. In this way, tilted homogeneous cells with different tilt angles were prepared. The (I) type surface treatment leads to a bulk tilt angle of about 60° (1 rad) with the normal to the surface [14] and the (II) type surface treatment gives higher tilt angles of 70–85° (1·2–1·5 rad). The (III) type surface treatment leads to lower bulk tilt angles, strongly dependent on the liquid crystal, as can be seen by comparing the results in [8] with the results in the present paper. The cells were filled with several different liquid crystal materials: NP 9A, NP 997, ZLI 1623 (E. Merck) and MBBA (Eastman Kodak), in the isotropic state. All the liquid crystals have $\Delta\varepsilon < 0$. The nematic–isotropic transition temperatures, as measured in the sample cells, are

Downloaded At: 09:23 26 January 2011

Values of $\bar{k}_{13}/k$ at 20°C and of fit parameters C and D.

Liquid crystal	T_{NI}/°C	T_c/°C	Cell geometry	Anchoring strength	$\bar{k}_{13}/k$	C	D
ZLI 1623	80	82	homogeneous, (I) type surface	Strong	1·7	2·0	−2·0
			homogeneous, (III) type surface [8]	Strong	1·7	2·0	−2·0
NP 9A	57	61	homogeneous, (III) type surfaces	Weak	−0·6	−0·9	1·6
			hybrid (surfactant/PVA) [16]	Strong	−0·6[a]	−0·8[a]	1·4[a]
NP 997	78	81	homogeneous, (I) type surfaces	Weak	1·8	1·85	−0·5
			homogeneous, (II) type surfaces	Weak	1·8	1·85	−0·6
			homogeneous, (III) type surfaces	Weak	1·7	1·8	−0·5
			hybrid (surfactant/PVA) [16]	Weak	1·7	1·7	−0·2
NP 8A	59	61	homogeneous, (III) type surfaces [8]	Strong	1·5	1·7	−1·2
			hybrid (surfactant/PVA) [16]	Weak	1·4	1·7	−1·8
MBBA	41·5	45	homogeneous, (III) type surfaces	Weak	−1·0	−1·0	0·2
	43·5	47	free surface [2]	Weak	−0·9	−0·9	0·2
	46·8	48	homogeneous, (I) type surfaces [3]	Weak	−0·8	−0·9	0·4
	46·8	48	homogeneous, (II) type surfaces [3]	Weak	−0·9	−1·0	0·4
	41·5	45	hybrid (lecithin/PVA) [16]	Weak	−0·75	−0·8	0·3

[a] New fit considering strong anchoring hypothesis.

listed in the table. The liquid crystals NP 9A, NP 997 and ZLI 1623 are provided by Merck with the surfactant ZLI 584 dissolved in them. In the filling process of a cell having SiO_x deposited surfaces with such a liquid crystal, two regions are obtained: an initial one of low tilt angle where the surfactant is present, and a second one of high tilt angle where the surfactant is missing, having been adsorbed by the surfaces of the first region. This last region is of (I) or (II) type or of planar (twisted) type, depending on the incident angle of the SiO_x deposition. The bulk tilt angle versus temperature for these liquid crystals was evaluated from measurements of the optical path difference between the ordinary and the extraordinary waves produced by the cell, using the tilting compensator of a Zeiss Amplival Pol U microscope. The temperature dependences of the refractive indices of the liquid crystals were measured by an independent method. For high tilt angles in samples of (I) and (II) type, the tilt angle was also evaluated by comparing the effective birefringence, introduced by the cell, to the birefringence in the same region, for the planar configuration obtained by applying an a.c. voltage of 50 V and 5 kHz. High tilt angles (greater thn 75°) were also measured by the rotating crystal method [15].

3. Results

The results for the measured tilt angles for MBBA and NP 9A with the (III) type surface treatment are presented in figures 1 and 2. The best fit curves are represented in the same figures and the fitting parameters obtained by the best fit are given in the caption of the respective figure. We notice that for these two liquid crystals, the bulk tilt angle/temperature dependence is quite different from that of the other liquid crystals with the same surface treatment, reported in [8]. For MBBA and NP 9A the bulk tilt angle decreases, tending to low values, while for the liquid crystals in [8], the bulk tilt angle increases from negative values to positive values, passing through a homeotropic alignment. As an example, in figure 3, this dependence for one of the liquid crystals studied in [8] (NP 997) and its best fit curves

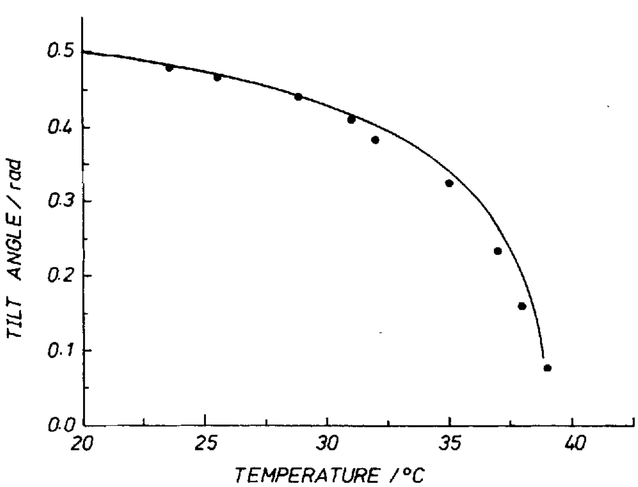

Figure 1. Average tilt angle, Φ_b, versus temperature for MBBA, (III) type surfaces. ●—experimental results. Best fit curve according to equation (8), $T_c = 45°C$, $A = 0{\cdot}8$, $B = 0{\cdot}15$, $C = -1{\cdot}0$, $D = 0{\cdot}2$, $\chi^2 = 6 \cdot 10^{-4}$, $\Phi_e = 0°$.

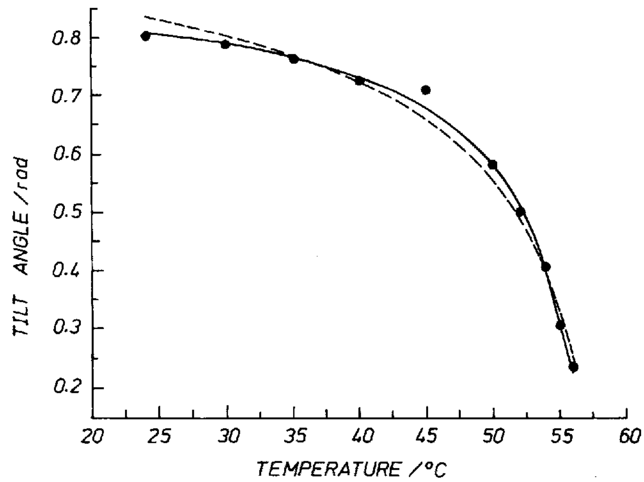

Figure 2. Average tilt angle, Φ_b, versus temperature for NP 9A, (III) type surfaces. ●—experimental results. Continuous curve – best fit curve according to equation (8), $T_c = 61°C$, $A = 0{\cdot}3$, $B = -0{\cdot}6$, $C = -0{\cdot}9$, $D = 1{\cdot}6$, $\chi^2 = 2 \cdot 10^{-4}$, $\Phi_e = 0°$. Dotted curve – best fit according to equation (1), $T_c = 61°C$, $\Phi_0 = 0{\cdot}644$, $C = -1{\cdot}1$, $D = 4{\cdot}3$, $\chi^2 = 9 \cdot 10^{-4}$.

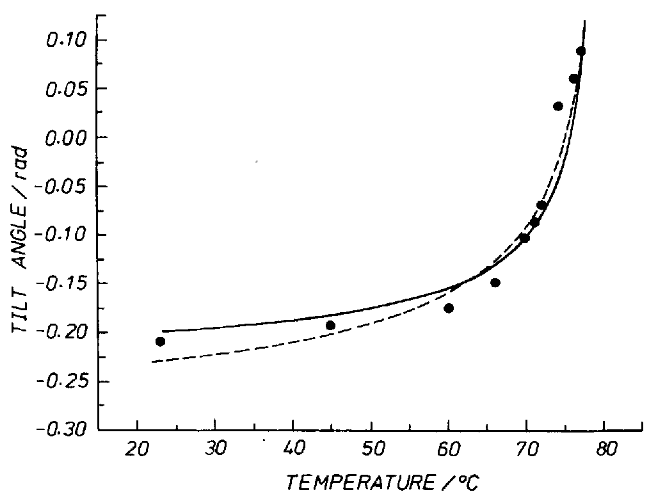

Figure 3. Average tilt angle, Φ_b, versus temperature for NP 997, (III) type surfaces. ●—experimental results. Continuous curve – best fit curve according to equation (8), $T_c = 82°C$, $A = 1{\cdot}4$, $B = -3{\cdot}4$, $C = 1{\cdot}8$, $D = -0{\cdot}5$, $\chi^2 = 9 \cdot 10^{-4}$, $\Phi_e = 0°$. Dotted curve – best fit according to equation (1), $T_c = 82°C$, $\Phi_0 = 0{\cdot}551$, $C = 2$, $D = -1{\cdot}8$, $\chi^2 = 7 \cdot 10^{-4}$.

Downloaded At: 09:23 26 January 2011

using not only equation (1), but also equation (8), respectively, are given. The best fit curve for MBBA and NP 9A leads to negative values of $\bar{k}_{13}/k$.

In figures 4 and 5, the experimental results obtained for the liquid crystals NP 997 and ZLI 1623 with the (I) and (II) type surfaces are given.

For weak anchoring, we observe that a negative argument of arccos function in equation (5) corresponds to Φ_e equal to 90°, and a positive one to Φ_e equal to 0° [11]. In the table, the values obtained for $(\bar{k}_{13}/k)$ at 20°C and the fit parameters C and D, for the liquid crystals studied are compared with those reported in other papers [8, 16].

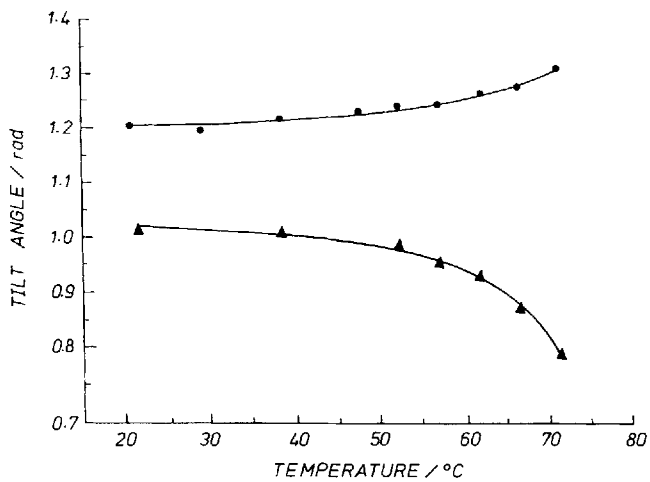

Figure 4. Average tilt angle, Φ_b, versus temperature for NP 997. ▲—experimental results for (I) type surfaces. Continuous curve – best fit curve according to equation (8), $T_c = 82$°C, $A = -3{\cdot}3$, $B = 2{\cdot}7$, $C = 1{\cdot}85$, $D = -0{\cdot}5$, $\chi^2 = 1 \cdot 10^{-4}$, $\Phi_e = 90°$. ●—experimental results for (II) type surfaces. Continuous curve – best fit curve according to equation (8), $T_c = 82$°C, $A = -3{\cdot}3$, $B = 2$, $C = 1{\cdot}85$, $D = -0{\cdot}6$, $\chi^2 = 4 \cdot 10^{-5}$, $\Phi_e = 90°$.

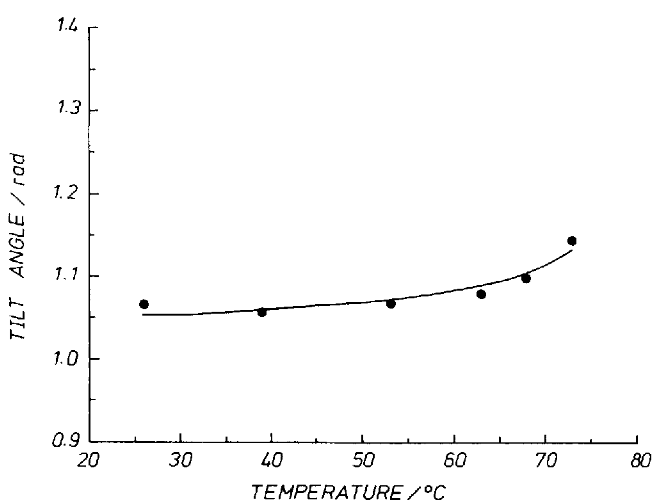

Figure 5. Average tilt angle, Φ_b, versus temperature for ZLI 1623, (I) type surfaces. ●—experimental results. Continuous curve – best fit curve according to equation (1), $T_c = 82$°C, $\Phi_0 = 1{\cdot}378$, $C = 2{\cdot}0$, $D = -2{\cdot}0$, $\chi^2 = 2 \cdot 10^{-4}$.

4. Discussion

Equations (1) and (8) contain a relatively large number of fitting parameters so that the tilt angle versus temperature can be fitted with several sets of fitting parameters for each anchoring hypothesis. However, from these parameters, two (C and D) refer to the liquid crystal and should lead to similar $\bar{k}_{13}/k$ values and temperature dependences in samples with the same liquid crystal, but different surface treatments. These criteria also enable us to choose between the two anchoring hypotheses, the strong anchoring usually involving a stronger temperature variation. The results for MBBA have been fitted only by means of equation (8). The fitting by means of equation (1) is not given because it leads to too strong a variation of $\bar{k}_{13}/k$ with temperature which cannot be found by analysing other experimental results obtained for different anchoring conditions. The same criterion of rate variation of $\bar{k}_{13}/k$ leads to our choice of weak anchoring for fitting the results in figure 4 and of strong anchoring in figure 5. Strong anchoring has to be rejected in order to interpret the results in figure 6, because it leads to an opposite variation of the bulk tilt angle with temperature.

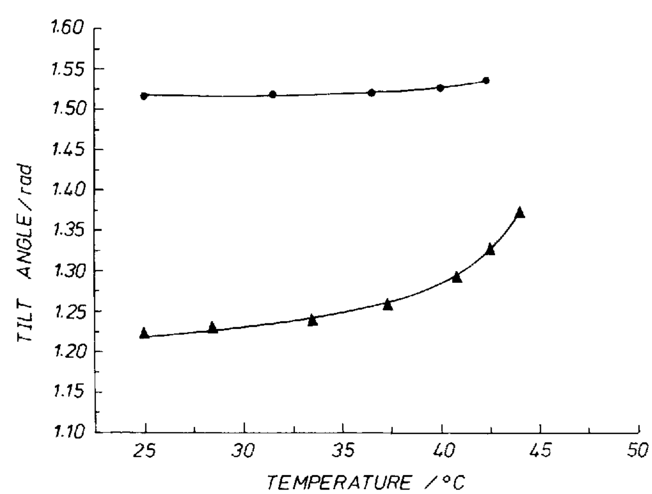

Figure 6. Average tilt angle, Φ_b, versus temperature for MBBA. ▲—experimental results for (I) type surfaces. Continuous curve – best fit curve according to equation (8), $T_c = 48$°C, $A = 0{\cdot}1$, $B = -0{\cdot}8$, $C = -0{\cdot}9$, $D = 0{\cdot}4$, $\chi^2 = 3 \cdot 10^{-5}$, $\Phi_e = 90°$. ●—experimental results for (II) type surfaces. Continuous curve – best fit curve according to equation (8), $T_c = 48$°C, $A = -0{\cdot}6$, $B = -0{\cdot}1$, $C = -1$, $D = 0{\cdot}4$, $\chi^2 = 2 \cdot 10^{-6}$, $\Phi_e = 90°$.

Downloaded At: 09:23 26 January 2011

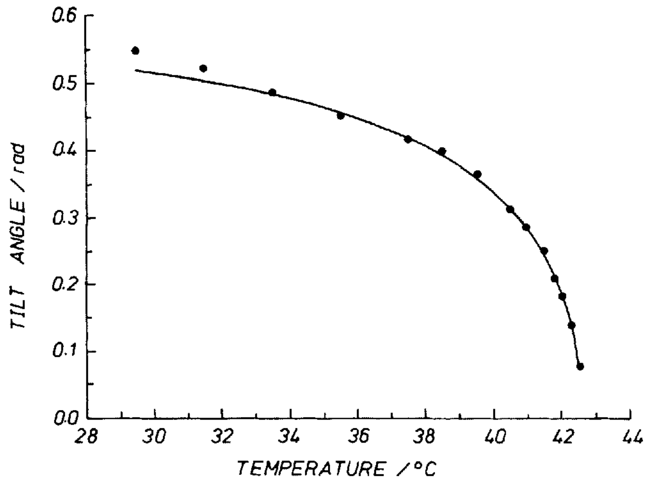

Figure 7. Average tilt angle, Φ_b, versus temperature for MBBA. ● — experimental results for the free surface. Continuous curve — best fit curve according to equation (8), $T_c = 47°C$, $A = 0{\cdot}6$, $B = 0{\cdot}2$, $C = -0{\cdot}9$, $D = 0{\cdot}2$, $\chi^2 = 1 \cdot 10^{-4}$, $\Phi_e = 0°$.

Another criterion for choosing adequate fitting parameters in the weak anchoring hypothesis is that for some surface treatments the Φ_e value is easily predicted. For example, we expect Φ_e to be 90° for (II) type surface treatment. In figures 6 and 7, the fits of experimental data from the literature for MBBA at the free surface [2], on (I) [3] and on (II) [3] type surfaces with the fitting parameters chosen taking into account the above requirement, are given. We arrive at the conclusion that, for MBBA at 20°C, $\bar{k}_{13}/k \approx -1$, instead of $\bar{k}_{13}/k \approx -1{\cdot}5$ as we found in [11]. The results of temperature induced surface transition measurements in a hybrid cell [16] confirm this assertion, as can be seen from the table. Some differences between the $\bar{k}_{13}/k$, C and D values, for the same liquid crystal, which are observed in the table can be explained either by the approximations contained in the theory (the uni-constant approximation; the neglecting of the surface micro-topography), or by experimental errors.

5. Conclusions

We remark that temperature induced surface transitions for the four liquid crystals studied are described well using the elastic model. As can be seen from the table, we could choose fitting parameters C and D, and consequently values of $(\bar{k}_{13}/k)$, as well as its type of temperature dependence, in good agreement for the same liquid crystal, independent of the cell geometry (tilted homogeneous, hybrid) and the surface treatment. Therefore, these experimental results provide new arguments for the validity of the elastic model for temperature induced surface transitions and permit a more reliable evaluation of the $\bar{k}_{13}/k$ ratio of elastic constants.

References

[1] Bouchiat, M. A., and Langevin-Crouchon, D., 1971, *Phys. Lett.*, **34A**, 331.
[2] Chiarelli, P., Faetti, S., and Fronzoni, L., 1983, *J. Physique*, **44**, 1061.
[3] Shimoda, S., Mada, H., and Kobayashi, S., 1979, *The Physics and Chemistry of Liquid Crystal Devices*, edited by G. Sprokel (New York: Plenum Press).
[4] Patel, J. S., and Yokoyama, H., 1993, *Nature*, **362**, 525.
[5] Flatisher, L., Komitov, L., Lagerwall, S. T., Stebler, B., and Strigazzi, A., 1992, *Molec. Crystals liq. Crystals*, **189**, 119.
[6] Di Lisi, G. A., Rosemblatt, C. Griffin, A. C., and Uma Hari, 1990, *Liq. Cryst.*, **7**, 353.
[7] Barbero, G., Beica, T., Alexe-Ionescu, A. L., and Moldovan, R., 1993, *Liq. Cryst.*, **14**, 1125.
[8] Barberi, R., Barbero, G., Giocondo, M., and Moldovan, R., 1994, *Phys. Rev. E*, **50**, 2093.
[9] Barbero, G., and Durand, G., 1993, *Phys. Rev. E*, **48**, 1942.
[10] Alexe-Ionescu, A. L., Barbero, G., and Durand G., 1993, *J. Physique II*, **3**, 1247.
[11] Beica, T., Frunza, S., Moldovan, R., and Ponti, S., 1995, *Phys. Lett. A*, **197**, 164.
[12] Shen, Y., 1989, *Liq. Cryst.*, **5**, 635.
[13] Rapini, A., and Papoular, M., 1969, *J. de Phys. Colloq.*, **30**, C4–54.
[14] Guyon, E., Pieranski, P., and Boix, M., 1973, *Lett. appl. eng. Sci.*, **1**, 19.
[15] Baur, G., Wittwer, V., and Berreman, D. W., 1976, *Phys. Lett. A*, **56**, 142.
[16] Moldovan, R., Tintaru, M., Frunza, S., and Beica T., 1995, *Rom. J. Phys.*, **40**, 605.

Downloaded At: 09:23 26 January 2011